Polarization Anisotropy and Valence Band Mixing in Semiconductor Quantum Wires

F. Vouilloz, D. Y. Oberli, M.-A. Dupertuis, A. Gustafsson, F. Reinhardt, and E. Kapon
Département de Physique, Ecole Polytechnique Fédérale de Lausanne, CH-1015 Lausanne, Switzerland
(Received 16 July 1996)

We have studied the effect of valence band mixing on the optical properties of semiconductor quantum wires by analyzing the luminescence polarization. Large polarization anisotropy is observed and directly compared to the effects predicted by a $\mathbf{k} \cdot \mathbf{p}$ model calculation of the valence band structure. [S0031-9007(97)02503-9]

PACS numbers: 78.55.Cr, 71.35.Cc, 73.20.Dx, 78.66.Fd

The electronic structure of spatially confined electrons in low-dimensional systems has been attracting considerable interest. In particular, the electronic and optical properties of semiconductors can be tailored in artificial nanostructures due to quantization of the electronic energy and emergence of strong excitonic features [1]. Enhancement of excitonic effects may be achieved in semiconductor quantum wires (QWRs) due to modifications of electron-hole Coulomb correlations and divergence of the one-dimensional (1D) joint density of states [2,3]. The band structure of 1D semiconductor QWRs has been studied theoretically and the prominent role of valence band mixing was described in model systems [4,5]. Unlike the case of quantum wells, the admixture of heavy hole (hh) and light hole (lh) states leads to modified energies of the optical interband transitions, which are tunable by the lateral confinement potential, and a redistribution of the oscillator strength. Moreover, it gives rise to intrinsic polarization anisotropy of the optical absorption spectra providing a unique way to gain insight into the nature of 1D valence band structures.

Despite the interest spurred on by these theoretical expectations the observation of the predicted features, i.e., optical anisotropy and sharp optical resonances, have been hampered by the technological challenge in producing QWR structures with two-dimensional (2D) confinement for both the ground state and excited states and with sufficiently small level broadening. The effect of 2D quantum confinement has been evidenced in the luminescence of QWR structures prepared by different approaches [6–9]. Study of the valence band mixing requires, however, the resolution and identification of several 1D valence subbands, imposing stronger constraints on the optical quality. Furthermore, anisotropy of optical interband transitions can also occur in the presence of strain, in samples with a strong surface corrugation, and in (110)-oriented quantum wells [10]. Initial observation of optical anisotropy in the absorption or emission of most types of QWR structures have been in fact affected by some of these invasive effects and, thus, cannot be directly compared to the predicted effects of 2D confinement on valence-band mixing.

In this Letter we report the observation of valence band mixing effects in the optical spectra of high quality 1D semiconductor QWRs. The origin of the optical transitions and their hh and lh character have been identified by performing photoluminescence experiments with circularly polarized light. The observed anisotropy in the linearly polarized excitation spectra of these wires is shown to arise solely from the 1D nature of the electronic band structure; it is directly compared to a detailed theoretical calculation of the strength of the optical transitions taking into account valence band mixing in actual QWR structures.

Photoluminescence (PL) and PL excitation (PLE) experiments with polarization analysis of the luminescence and excitation were performed on QWRs of different sizes. GaAs-QWRs embedded in $Al_{0.3}Ga_{0.7}As$ were grown by low pressure organometallic chemical vapor deposition (OMCVD) on grooved (001) GaAs substrates, with the wires oriented in the $[1\bar{1}0]$ direction [11]. A typical cross-sectional view of the QWR heterostructure is shown in the transmission electron microscope (TEM) micrograph of Fig. 1. We have studied three samples, each consisting of a 0.5 μm pitch lateral array of single QWRs of different sizes. The nominal GaAs layer thicknesses were 5, 2.5, and 1.5 nm, resulting in a thickness at the crescent center of 14.1, 8.8, and 4.1 nm, respectively.

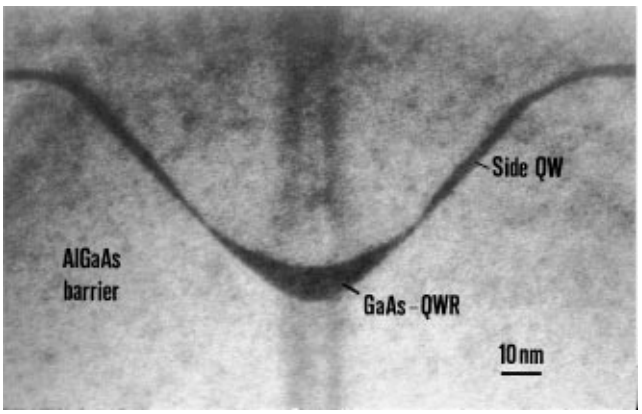

FIG. 1. TEM micrograph showing a cross-sectional view of the QWR region. Nominal GaAs thickness is 2.5 nm, and GaAs crescent is 8.8 nm thick at its center.

 0031-9007/97/78(8)/1580(4)$10.00

The samples were mounted in a helium-flow cryostat and kept at 8 K. The optical spectra were obtained in a pseudo-backscattering geometry from the (001) plane using polarized light from an argon-ion laser (2.4 eV) for the PL measurements and from a titanium-sapphire laser for the PLE experiments. The excitation light was focused onto a spot approximately 35 μm in diameter; typical power densities of 25 W/cm^2 were used. For linear polarization measurements, perpendicular (parallel) refers to the [110] ([1$\bar{1}$0]) direction. For circular polarization measurements the helicity of the exciting light (σ^+) was fixed. The helicity of the luminescence was analyzed by combining a quarter-wave plate and a linear polarizer in order to transmit the σ^+ or the σ^- component. The spectral resolution was 0.8 meV.

A typical PL spectrum for a QWR sample is displayed in Fig. 2. On the low-energy end of the spectrum, the peak at 1.568 eV is assigned to the luminescence of the QWR. The broader peak at 1.707 eV corresponds to that of the side quantum wells and the weaker peak at 1.915 eV is due to recombinations in the AlGaAs barrier material. The PL full width at half maximum (FWHM) of the QWR peak ranges from 5.4 to 6.9 meV and the FWHM of the first PLE peak ranges from 3.7 to 12.0 meV for the three samples investigated. We found that the integrated QWR luminescence varies linearly with excitation power density between 1 and 10^3 W/cm^2 [12], which supports the intrinsic and excitonic nature of the recombination process [13]. Excitonic effects already play a major role in the optical-absorption spectra of 2D systems [14]. Moreover, the Sommerfeld factor was calculated [2] and found much smaller than unity for a direct allowed interband transition in a 1D system, in striking contrast to the 3D and 2D cases. For these reasons, we believe that the optical spectra are fully dominated by the excitonic nature of the optical transitions.

The inset in Fig. 2 shows the monotonous decrease of the energy Stokes shift and the FWHM of the lowest-energy PLE peak with increasing crescent thickness. The small Stokes shifts (3.6–8.5 meV) and PLE linewidths attest to the high quality of these wires.

The PLE spectra of two of the samples, with 2.5 and 1.5 nm QWR nominal thickness, are shown in Fig. 3. The linearly polarized PLE spectra of the 5-nm QWR sample resemble those of the 2.5 nm sample, except that the peaks are shifted to lower energies and their spacings are smaller. The dependence of the optical spectra on the orientation of the polarization reveals a striking polarization anisotropy. The PLE spectra show up to seven peaks corresponding to excitonic transitions of 1D quantum-confined energy levels. A decrease of the wire thickness leads to a blueshift of the ground state transition, e_1-h_1, that increases from 1.538 eV for the 5-nm QWR to 1.634 eV for the 1.5-nm QWR. In addition, the energy separation between the e_n-h_n transitions increases for thinner wires; the separation between the e_1-h_1 and e_2-h_2 transitions is 15 meV for the 5-nm QWR and 26 meV for the 1.5-nm QWR.

For a quantitative understanding of the optical spectra we performed calculations of the confinement energies for a 2D finite potential-well model beyond the approximation of parabolic valence bands in order to include the degeneracies and band-mixing interactions of the $J = \frac{3}{2}$ multiplet of the valence-band states. It is based on a

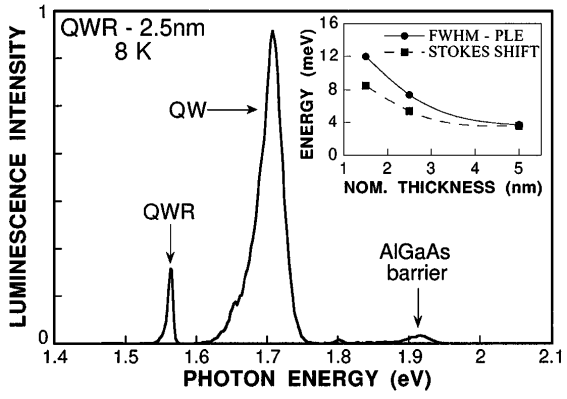

FIG. 2. PL spectrum of a QWR sample with a nominal GaAs thickness of 2.5 nm excited with the 2.4 eV line of an Ar^+ laser. Inset shows FWHM of the first PLE peak and Stokes shift versus the nominal layer thickness.

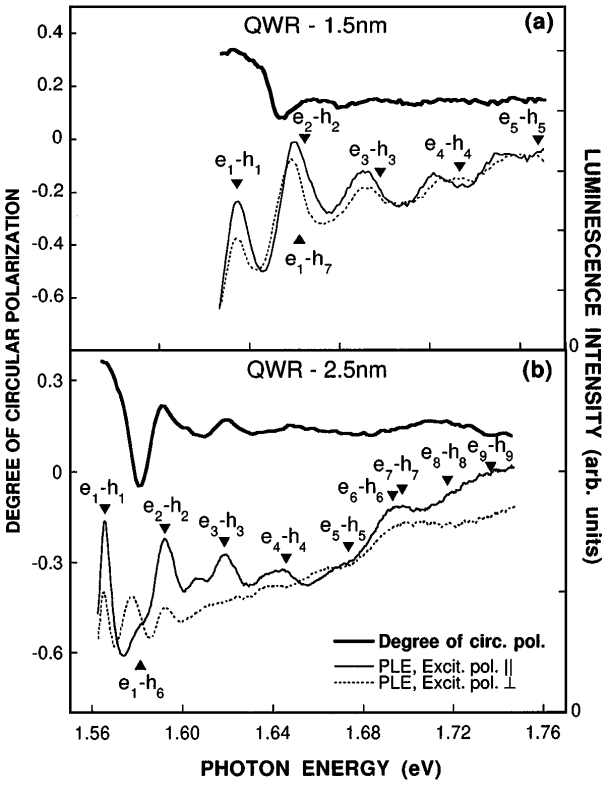

FIG. 3. Degree of circular polarization (see text for definition) and linearly polarized PLE spectra for QWR samples with a nominal GaAs thickness of (a) 1.5 nm and (b) 2.5 nm. Detection wavelength is set at the maximum of PL line.

solution of the 2D Schrödinger equation in the single-particle approximation using the 4×4 $\mathbf{k} \cdot \mathbf{p}$ Hamiltonian [15] and a potential profile extracted from the TEM micrograph of the sample. In Fig. 3, we indicated the position of the calculated optical interband transitions. In order to compare the observed 1D excitonic transitions with the calculated interband transitions, we introduced a rigid energy redshift of each series of optical transitions e_n-h_n. The overall agreement with the theoretical calculations was very good for all three investigated samples. Remaining differences may be attributed in one part to a slightly different wire cross section in the sample's piece used for the TEM study and in another part to additional excitonic effects, which were not included.

The influence of the lateral confinement in the QWRs on the optical properties manifests itself by a linear polarization dependence of the PLE spectra. Clear optical anisotropy in absorption is observed for all three samples. The effect is particularly pronounced for the 2.5-nm QWR and for the 5-nm QWR where a clear crossing in the PLE spectra occurs for the second 1D excitonic transition when measured with orthogonal polarizations. This feature is less pronounced in the PLE spectra of the thinnest 1.5-nm QWR. We also find that the emission from the wire is polarized. A mean value of 10% for the anisotropy is measured across the PL line with a selective photoexcitation in the wire.

The observed optical anisotropy is well described by valence band mixing resulting in an admixture of both hh and lh bulk states at any point of the Brillouin zone [4,5]. Optical anisotropy can be present, however, in the absence of any quantum confinement. Therefore, it is important to evaluate the strength of the optical transitions and their anisotropies on the basis of 2D confinement alone. The calculated squared optical matrix elements are displayed in Fig. 4 for the 2.5-nm QWR sample. All the main features of the experimental PLE spectra are remarkably reproduced in Fig. 4: The dominance of the optical transitions e_n-h_n in parallel polarization is clearly evidenced, whereas transitions with nonconserving subband indices are strongly suppressed. Furthermore, the peak labeled e_1-h_6 carries a large oscillator strength and dominates in perpendicular polarization resulting in a large polarization anisotropy. This latter feature is a vivid signature of valence-band mixing and originates from the contribution to the valence subband of Bloch states having a dominant lh character [4,5]. Our calculation confirms this expectation with a value of 70% lh character for that excited valence state (see Table I). In addition the lh part of the wave function of that $n = 6$ state has its maximum at the center of the wire and, thus, this state mainly couples to the $n = 1$ conduction subband due to a large overlap [16]. The weakness of the optical anisotropy in the optical spectra of the 1.5-nm QWR is due to the fortuitous superposition of two optical transitions e_2-h_2 and e_1-h_7 and to the larger elongation of its crescent shape. Within the framework of an

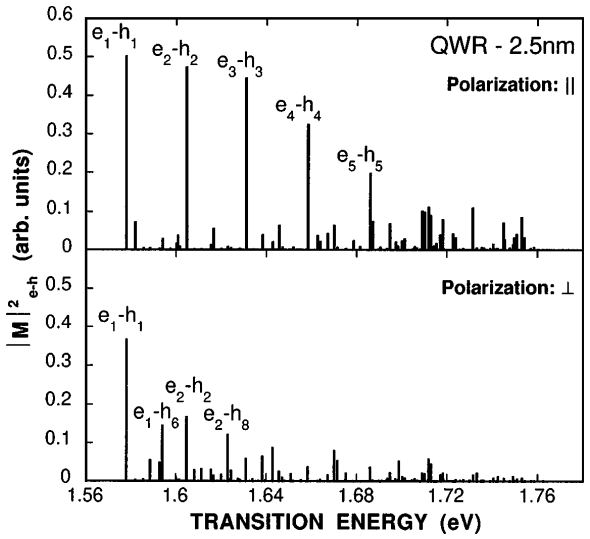

FIG. 4. Square of the optical matrix elements for interband transitions $e_i - h_j (1 \leq i, j \leq 10)$ calculated at $k = 0$ for the 2.5-nm QWR (no adjustable parameters). Major transitions are labeled according to the indices of the participating electron and hole subbands.

adiabatic decoupling of the 2D potential, this occurs when the transverse potential splits the first hh and lh subbands by an amount equal to the energy separating 1D electron subbands imparted by the lateral potential [17]. In comparing the relative intensities of PLE spectral features, we have implicitly assumed a one-to-one correspondence to absorption peaks as PLE spectra of quantum wells show a close resemblance to calculated absorption spectra [18]. We note that an exact correspondence holds if the relaxation rate from the excited state towards the emitting state dominates over nonradiative recombination rates.

We shall now discuss alternative causes to polarization anisotropy unrelated to 2D confinement. Specific morphologies of a quantum well interface which contains partially ordered and elongated monolayer islands are known to be a source of optical anisotropies unrelated to any lateral confinement [19]. Another important source of anisotropy is caused by electromagnetic polarization effects on samples presenting at the surface a dielectric grating [20,21]. QWRs prepared by etching have given rise to large optical anisotropies although unrelated to the extent of any lateral confinement [8,20,22]. Intrinsic optical anisotropy can also appear in GaAs heterostructures when the orientation of the quantum well departs from the [100] symmetry axis [10]. Finally, localization of excitons on interfacial defects can strongly affect any polarization analysis based on extended states. We checked

TABLE I. Percentage of lh character for valence subbands at the zone center for the 2.5-nm QWR.

Subband	h_1	h_2	h_3	h_4	h_5	h_6	h_7	h_8
% lh	10	33	45	53	49	70	46	30

that the polarization anisotropy in the PLE spectra was independent of the detection wavelength in contrast to that of the PL spectra which is strongly affected by excitation wavelength and localization effects. We also performed all measurements on planarized parts of the samples freed from surface grating effects.

To further investigate and confirm the nature of the valence states involved in the observed optical transitions, we used circularly polarized light to excite the QWR luminescence. Assuming no electron spin relaxation [23], this leads to circular polarization of the PL, which depends on the initial conduction and valence states. The measured degree of circular polarization $\mathcal{P} = (I^+ - I^-)/(I^+ + I^-)$, where $I^+(I^-)$ is the $\sigma^+(\sigma^-)$ circularly polarized luminescence intensity, is also shown in Fig. 3.

In the energy range $E_{\text{exc}} < e_1 - \text{“lh”}_1$ only electrons from the lowest valence subbands are excited to the conduction subband. Here “lh”$_1$ refers to the first valence subband displaying a dominant light hole character. Since the first valence subbands have a dominant hh character the resulting $\mathcal{P}$ is positive, close to 35% at the e_1-h_1 transition. For an excitation energy approaching the e_1-“lh”$_1$ transition, the electrons from the valence subband with strong lh character start to contribute to the luminescence. These electrons are created with $s = +\frac{1}{2}$ and are associated with a negative $\mathcal{P}$ at the e_1-h_1 transition. As the first valence subbands contribute to a positive $\mathcal{P}$, the joint density of states (JDOS) for the transition e_1-“lh”$_1$ has to be very high to compensate for it giving rise to a decrease in $\mathcal{P}$. This is further supported by our calculation of the valence band structure: A negative “lh” mass at the center of the Brillouin zone is found in all the QWRs investigated [16]. This effect explains the pronounced dip located at the e_1-“lh”$_1$ transition in the polarization spectrum of Fig. 3(b). As the excitation energy increases, the JDOS for the e_1-“lh”$_1$ transition falls down and the net polarization increases again. For still higher excitation energies ($E_{\text{exc}} < e_1 - \text{“lh”}_1$) electrons from other valence subbands also appear in the conduction subbands. Because the depolarization increases with the kinetic energy of photocreated electrons [23], these electrons will only weakly contribute to the polarization and, thus, the circular polarization curve features only small amplitude modulations for optical transitions e_n-h_n with $n > 2$.

In summary, this study of high quality semiconductor QWRs has revealed several features specific to quantum confinement in two directions: the formation of well resolved 1D subbands with energy separation as large as 30 meV and the predicted polarization anisotropy of optical transitions due to valence band mixing. A detailed $\mathbf{k} \cdot \mathbf{p}$ theoretical analysis has confirmed the key role played by valence-band mixing in the optical spectra and proved its relevance. The effect of disorder on the excitonic emission in strongly confined quantum systems remains to be evaluated in relation to polarization anisotropy and should stimulate further theoretical studies.

We wish to thank P. Ils and U. Marti for preparing the patterned substrates and G. Biasiol for his contribution to the OMCVD growth of the samples. We are grateful to B. Deveaud for a critical reading of the manuscript. This work was supported in part by the Fonds National Suisse de la Recherche Scientifique.

[1] See, e.g., W. Jaskólski, Phys. Rep. **271**, 1–66 (1996); in *Proceedings of the 4th International Conference on Optics of Excitons in Confined Systems, Cortona* [Nuovo Cimento Soc. Ital. Fis. **17D**, 11–12 (1995)].
[2] T. Ogawa and T. Takagahara, Phys. Rev. B **44**, 8138 (1991); S. Glutsch and F. Bechstedt, Phys. Rev. B **47**, 4315 (1993).
[3] F. Rossi and E. Molinari, Phys. Rev. Lett. **76**, 3642 (1996).
[4] U. Bockelmann and G. Bastard, Europhys. Lett. **15**, 215 (1991).
[5] D. S. Citrin and Yia-Chung Chang, Phys. Rev. B **43**, 11 703 (1991); P. C. Sercel and K. J. Vahala, Phys. Rev. B **44**, 5681 (1991).
[6] H. Akiyama, T. Someya, and H. Sakaki, Phys. Rev. B **53**, R4229 (1996).
[7] E. Kapon *et al.*, Phys. Rev. Lett. **63**, 430 (1989); R. Rinaldi *et al.*, Phys. Rev. B **50**, 11 795 (1994).
[8] L. Birotheau *et al.*, Appl. Phys. Lett. **61**, 3023 (1992).
[9] J. Bloch, U. Bockelmann, and F. Laruelle, Europhys. Lett. **28**, 501 (1994).
[10] Y. Kajikawa, Phys. Rev. B **47**, 3649 (1993), and references therein.
[11] A. Gustafsson, F. Reinhardt, G. Biasiol, and E. Kapon, Appl. Phys. Lett. **67**, 3673 (1995).
[12] Carriers were photoexcited into the wire by using energy-selective excitation.
[13] J. E. Fouquet, IEEE J. Quantum Electron. **22**, 1799 (1986).
[14] R. C. Miller and D. A. Kleinman, J. Lumin. **30**, 520 (1985), and references therein.
[15] J. M. Luttinger, Phys. Rev. **102**, 1030 (1956).
[16] A larger account of our calculations will be published elsewhere.
[17] D. Y. Oberli, F. Vouilloz, M.-A. Dupertuis, C. Fall, and E. Kapon, Nuovo Cimento Soc. Ital. Fis. **17D**, 1641 (1995).
[18] R. Winkler, Phys. Rev B **51**, 14 395 (1995).
[19] G. Bauer and H. Sakaki, Phys. Rev. B **44**, 5562 (1991).
[20] M. Kohl, D. Heitmann, P. Grambow, and K. Ploog, Phys. Rev. Lett. **63**, 2124 (1989).
[21] U. Bockelmann, Europhys. Lett. **16**, 601 (1991).
[22] P. Ils *et al.*, Phys. Rev. B **51**, 4272 (1995); H. Lage *et al.*, Phys. Rev. B **44**, 6550 (1991).
[23] A. Twardowski and C. Hermann, Phys. Rev. B **35**, 8144 (1987).